NASA Technical Memorandum 79157

EFFECT OF SHOCKS ON FILM COOLING OF A FULL SCALE TURBOJET EXHAUST NOZZLE HAVING AN EXTERNAL EXPANSION SURFACE

David M. Straight
Lewis Research Center
Cleveland, Ohio

Prepared for the
Fifteenth Joint Propulsion Conference
cosponsored by the AIAA, the SAE, and the ASME
Las Vegas, Nevada, June 18-20, 1979

EFFECT OF SHOCKS ON FILM COOLING OF A FULL SCALE TURBOJET EXHAUST NOZZLE HAVING AN EXTERNAL EXPANSION SURFACE

David M. Straight
NASA-Lewis Research Center
Cleveland, Ohio

Abstract

Cooling is one of the critical technologies for efficient design of exhaust nozzles, especially for the developing technology of nonaxisymmetric (2D) nozzles for future aircraft applications. Several promising 2D nozzle designs have external expansion surfaces which need to be cooled. Engine data are scarce, however, on nozzle cooling effectiveness in the supersonic flow environment (with shocks) that exists along external expansion surfaces. This paper will present experimental film cooling data obtained during exploratory testing with an axisymmetric plug nozzle having external expansion and installed on an afterburning turbojet engine in an altitude test facility. The data obtained shows that the shocks and local hot gas stream conditions have a marked effect on film cooling effectiveness. An existing film cooling correlation is adequate at some operating conditions but inadequate at other conditions such as in separated flow regions resulting from shock-boundary-layer interactions.

Nomenclature

h_f	convection heat transfer coefficient (Eq. (11))
K_f	film thermoconductivity
M	mass flux ratio $(\rho V)_C/(\rho V)_G$
M_C	coolant Mach number
M_G	hot gas Mach number
NPR	nozzle pressure ratio, P_{T7}/P_o
P_o	nozzle exit static pressure (Altitude chamber)
Pr	Prandtl number
P_S	static pressure
P_T	hot gas total pressure, local
P_{T7}	hot gas total pressure, average at nozzle inlet
Q_1	radiation heat flux, hot gas to wall (Eq. (7))
Q_2	convection heat flux, wall to cooling film (Eq. (8))
Q_3	radiation heat flux, wall to ambient (Eq. (9))
R	recovery factor (Eq. (4))
R_1	radius of plug at cooling slot exit
Rex	length Reynolds number (Eq. (12))
S	cooling slot step height
$\overline{T_7}$	average hot gas total temperature at nozzle inlet
T_{amb}	ambient temperature (Altitude chamber wall)
T_{aw}	adiabatic wall temperature (Eq. (10))
T_c	coolant total temperature
T_f	film temperature $(T_{aw} + T_W)/2$
T_G	hot gas driving temperature
T_{GL}	local hot gas driving temperature
$\overline{T_R}$	hot gas recovery temperature, $f(\overline{T_7})$
T_{RC}	coolant recovery temperature (Eq. (5))
T_{RG}	hot gas recovery temperature (Eq. (3))
T_{RL}	local hot gas recovery temperature
T_{SC}	coolant static temperature
T_{SG}	hot gas static temperature
T_{TG}	hot gas total temperature
T_W	measured wall temperature
V_C	coolant velocity at slot exit
V_G	hot gas velocity
V_M	film velocity (Eq. (14))
W_A	engine inlet airflow
W_C	coolant slot airflow
W_G	hot gas flow at nozzle inlet
X	length from cooling slot
X_{eff}	effective length from cooling slot (Eq. (2))
α	half angle of plug
β	boat-tail angle of primary shroud
γ	ratio of specific heats
ϵ_F	flame emissivity
ϵ_W	wall emissivity
η	film cooling effectivess (Eq. (1))
μ_f	film viscosity
ρ_f	film density
ρ_c	coolant density
ρ_G	hot gas density
σ	Stefan - Boltzmann Constant

Subscripts:

(n)	measuring station along cooled surface
max.	maximum

Introduction

Extension of the data base in cooling technology is needed for the design of advanced exhaust nozzles. This is especially true for nonaxisymmetric concepts which have received considerable attention in recent years for application to advanced tactical aircraft.[1] The potential advantages of nonaxisymmetric nozzles for improved aircraft performance, maneuverability and survivability may be penalized by increased nozzle weight and cooling requirements because of the change in shape from the conventional round exit to two-dimensional (2D) exits.

Figure 1 presents three basic types of nonaxisymmetric nozzles currently being considered. The concepts range from the all internal expansion 2D-CD (Fig. 1(a)) to the partial-external-expansion

twin throat 2D plug (Fig. 1(b)) and the single ramp concept (Fig. 1(c)). All three concepts have increased surface areas that have to be cooled. Wind tunnel tests and system studies[2,3] have shown that nonaxisymmetric nozzles with a portion of the expansion along external surfaces (Figs. 1(b) and (c)) have potential advantages when integrated with an airframe. The shocks that occur along external free expansion surfaces, however, affect the heat transfer characteristics.[4]

In an effort to reduce the cooling flow requirements, more complex but more effective cooling systems are being considered (Fig. 2). The cooling methods range from simple light weight single wall film cooling at the top of Fig. 2 through two wall convection cooling to the most complex and usually heavier three wall combination of impingement and film cooling shown at the bottom of the figure. Film cooling, however, is an important part of most cooling systems because the most effective use of the spent coolant after being used for convection or impingement cooling is to direct the flow over the surface as a film wherever possible.

Experimental data obtained with a convectively air cooled axisymmetric plug nozzle (external expansion) on an afterburning turbojet agreed reasonably well with predictions.[5] The effect of shocks are not as pronounced when the coolant and hot gas are separated by a wall (convection cooling) which prevents entrainment of hot gas into the coolant flow as is the case with film cooling. A modification to the plug where the plug was partially film cooled to save weight and coolant pressure loss resulted in large variations in plug wall temperatures as nozzle pressure ratio changed.[4] These variations were attributed to shock wave patterns which change with nozzle pressure ratio.

Film cooling, although the most common cooling method in use for exhaust nozzles, is probably the least understood of the cooling methods for a supersonic flow with shocks environment, and engine data which include the effects of hot gas temperature gradients are scarce. The purpose of this paper is to provide some additional engine data to narrow this technology gap.

Results from several investigations using models, components, or heat transfer rigs have been published which illustrate some of the film cooling phenomena that also occur in engine tests. These investigations also provide analytical approaches for data analysis. Results from tests with a model of a plug nozzle[6] showed poor correlation of supersonic data at some conditions with a correlation derived from subsonic rig tests.[7] Results from a film cooled axisymmetric parallel diffuser model[8] and along a flat plate in a supersonic rig test[9] show differences between subsonic and supersonic results when using a downstream distance parameter for correlating film effectiveness. The downstream distance parameter was successful for correlating subsonic combustor rig results[10] and is currently used by designers of film cooled exhaust nozzle hardware[11] for both subsonic and supersonic flow. Both subsonic and supersonic data are compared with this same parameter in this paper.

The axisymmetric plug nozzle previously tested[4,5,12] was modified again to film cool the entire plug by air flowing from a slot located near the nozzle throat. The testing was completed in October 1978 at the NASA Lewis Research Center. Typical data sets were processed for comparison with the existing correlations and the results are presented. Some of the variables that need to be defined for improved analytical models are identified.

Apparatus

A schematic of the axisymmetric plug nozzle used for the film cooling experiment is shown in Fig. 3. The nozzle assembly was attached to the afterburner of a J85 turbojet engine which has a rated airflow of 44 pounds per second.

Two fixed area primary shrouds were used in this program to provide a simulation of the minimum area setting (nonafterburning) and the maximum area setting (maximum afterburning) of a variable area nozzle required for the afterburning turbojet. With the maximum area shroud (large primary), however, the full range of afterburning from maximum temperature rise ($\overline{T_7}$ = 3500° R) to zero temperature rise ($\overline{T_7}$ = 1180° R) could be obtained. Data were obtained at three afterburning levels plus nonafterburning. The small primary shroud could only be used nonafterburning ($\overline{T_7}$ = 1750° R). Use of both shrouds permitted evaluation of the effect of primary flow angle (function of primary boat-tail angle) as well as hot gas temperature variables on film cooling effectiveness.

Cooling air was supplied to the supporting struts from a facility air supply system at near ambient temperatures. The struts and forward portion of the plug were convectively cooled. After cooling the struts and front portion of the plug the cooling air was discharged through a film cooling slot 2.6 inches from the primary throat and then film cooled the remainder of the plug (24.5 in.). The coolant slot was designed so that supersonic slot exit velocities could be obtained at high coolant flow rates (isometric view in Fig. 3). The plug was truncated at 60 percent of a full length cone. The film-cooled portion of the plug was insulated with high temperature insulation to minimize heat flow to the interior of the plug which improves the accuracy of wall-radiation-correction heat-balance calculations.

Thirteen measuring stations were located downstream of the cooling slot. Three wall temperatures (0°, 30°, 60° circumferential positions) and, two wall static pressures (10°, 90° circumferential positions) were located at each station and averaged at each station for input to the film cooling data analysis. Other measurements were made for determining coolant flow rate, temperature and total pressure at the inlet to the cooling slot. Engine airflow, fuel flow and nozzle inlet total pressure were measured for determining hot gas flow conditions. Nozzle inlet total temperature was obtained from an afterburner temperature rise calibration made in a previous test program using water cooled nozzles.

Two traversing probes were mounted on support beams, one on each side of the nozzle such that radial total pressure and temperature surveys of the hot gas stream including the boundary layer (cooling air film) near the plug wall could be measured at various positions downstream from the primary shroud. The temperatures were measured with a 60 percent iridium - 40 percent rhodium versus iridium thermocouple system. Both probes were

water cooled so that measurements could be made up to maximum afterburning temperatures. A photograph of the installation in an altitude test facility is shown in Fig. 4.

Film Cooling Correlation

The general form of film cooling effectiveness expressed as a function of the downstream distance parameter for correlating data can be expressed as follows:

$$\text{(Effectiveness)} = f\ \text{(Distance)}$$

$$\eta = \frac{(T_G - T_{aw})}{(T_G - T_c)} = f\left(\frac{X}{MS}\right) \qquad (1)$$

Film cooling of the plug in this experiment occurred in a high velocity hot gas environment such that compressible flow equations and variable gas properties were used in defining both correlating parameters, X/MS and η. In addition, radiation corrections to the measured wall temperature were computed to obtain the adiabatic wall temperature needed in the film cooling effectiveness parameter. A brief discussion of the equations used for the effectiveness and distance parameters and method of solution is presented in the following paragraphs. The wall radiation and probe corrections are also discussed.

Downstream Distance Parameter

The hot gas stream expands freely from the nozzle inlet total pressure P_{T7} to the exit static pressure, P_o, along the external film-cooled conical expansion surface. Because of the accelerating flow, the hot gas static pressure, static temperature, and velocity vary along the flow path. The coolant to hot gas mass flux ratio, M, therefore, varied at each measuring station (n) and is a function of local measured static pressure. Local static temperature, density, and velocity of the hot gas are determined from nozzle inlet total pressure and total temperature assuming isentropic expansion to local static pressure, $P_{S(n)}$, along the plug wall. Variable specific heat ratios (instantaneous values) are computed as a function of total temperature, fuel-air ratio, and $P_{S(n)}/P_{T7}$.[13]

The coolant mass flux $(\rho v)_c$, was evaluated at slot exit conditions from measured coolant total pressure and temperature at the slot inlet and static pressure inside the slot near the exit. The compressible flow equations were also used for this computation.

The distance from the slot, X, also needs a definition because the surface being cooled is a cone instead of a flat plate as is used in most rig experiments. An effective length, X_{eff} was used:

$$X_{eff(n)} = X_{(n)} - \frac{X^2_{(n)}\ \text{Sin}\ \alpha}{2\ R_1} \qquad (2)$$

The effective length at a station (n) is the length of an equivalent cylindrical surface having the same surface area and a diameter equal to the plug diameter at the cooling slot exit.

The cooling slot height, S, was chosen to be the step height (0.13 in.) which includes the wall thickness of the slot lip.[9]

Film Cooling Effectiveness Parameter

The hot gas Mach number varied over a wide range from subsonic to about 2.7 depending on test condition and distance downstream from the nozzle throat. The theoretical flat plate adiabatic wall temperature with no coolant film is equal to the recovery temperature of the hot gas and is used for the hot gas driving temperature, T_G, in the film cooling effectiveness parameter (Eq. (1)) for supersonic flow.[14] The recovery temperature is:

$$T_{kG(n)} = T_{SG(n)}\left[1 + R\left(\frac{\gamma - 1}{2}\right) M^2_{G(n)}\right] \qquad (3)$$

Where the recovery factor, R, is usually set equal to the cube root of Prandtl number for turbulent flow. Prandtl number was nearly constant and R was initially set equal to a constant (0.89).

Test runs at most nonafterburning conditions in this experiment included a run with zero coolant flow which permitted experimental determiniation of the actual recovery factor[15] which is defined as:

$$R = \frac{T_{aw} - T_{SG}}{T_{TG} - T_{SG}} \qquad (4)$$

Where T_{SG} is the hot gas static temperature, T_{aw} is the measured wall temperature corrected for radiation, and T_{TG} is measured (equal to turbine exit station with no afterburning).

Improvements in data correlation when using experimental Recovery Factors are discussed in a later section.

The coolant temperature, T_c in Eq. (1) was also replaced by the coolant recovery temperature, T_{RC}, because of supersonic coolant velocities at some test conditions.

$$T_{RC} = T_{SC}\left[1 + R\left(\frac{\gamma - 1}{2}\right) M^2_c\right] \qquad (5)$$

The Recovery Factor, R, was assumed constant (0.89) in Eq. (5) and the other terms T_{SC} and M_c were computed from coolant measurements.

Wall Radiation Corrections

The film cooling effectiveness parameter (Eq. (1)) is sensitive to temperature levels especially when the temperature difference terms are small. Corrections for thermal radiation become significant especially at high wall temperatures where radiation corrections on the measured plug wall temperatures can be several hundred degrees. Small temperature differences also occur for low or zero coolant flow runs and radiation corrections, although much smaller, are still needed.

A heat balance on the wall was assumed wherein the hot-gas-to-wall radiation, Q_1, was equal to the sum of the wall-to-coolant-film convection Q_2, and the wall-to-ambient radiation, Q_3.

$$Q_1 = Q_2 + Q_3 \qquad (6)$$

Where:

Radiation from hot gas to wall,

$$Q_1 = \left(\frac{1 + \epsilon_W}{2}\right) \sigma \epsilon_F T_G^{1.5} \left(T_G^{2.5} - T_W^{2.5}\right) \quad (7)$$

Convection from wall to cooling air film (or to hot gas if no coolant flow)

$$Q_2 = h_f (T_W - T_{aw}) \quad (8)$$

Radiation from wall to ambient (altitude chamber walls).

$$Q_3 = \epsilon_W \sigma \left(T_W^4 - T_{amb}^4\right) \quad (9)$$

Q_1, and Q_3, were determined directly from experimental measurements of $T_{W(n)}$, T_{amb}, and the calibrated hot gas temperature, T_7. The wall emissivity, ϵ_W, was assumed constant (0.75) and the flame emissivity, ϵ_F was computed as a function of pressure, fuel-air ratio, beam length and flame temperature.[16] A view factor of 1 was used for Q_3. The heat flux through the insulated wall to the interior of the plug was assumed equal to zero.

Equations (6) to (9) may then be solved for the adiabatic wall temperature.

$$T_{aw} = T_{W(n)} + \left(\frac{Q_3 - Q_1}{h_f}\right) \quad (10)$$

Where the remaining variable to be defined is the convection heat transfer coefficient, h_f.

The local heat transfer coefficient was calculated using the standard flat-plate correlation for turbulent flow

$$h_f = 0.0296 \frac{k_f}{X_{eff}} Rex^{0.8} Pr_f^{1/3} \quad (11)$$

Where fluid properties were evaluated at a film temperature, T_f, which was an average of the adiabatic wall temperature, T_{aw} and the wall temperature, T_W. Evaluation f the length Reynolds number, Rex, requires knowledge of the local cooling film conditions; that is, pressure, temperature and velocity which was also based on T_f. An iterative solution is required because the adiabatic wall temperature being sought is also needed for fluid properties and Rex in Eq. (11) where:

$$Rex = \frac{\rho_f V_M X_{eff}}{\mu_f} \quad (12)$$

Instead of using the method of Clark and Lieberman[16] for determining film velocity, a simplified mixing model similar to that for free jets[17] was chosen. The mixing model assumed that the rate of velocity change of the cooling film with increase in distance from the cooling slot was directly proportional to the rate of temperature change. With this assumption, both temperature and velocity change in proportion to the entrainment rate of hot gas into the cooling film.

The local adiabatic wall temperature (film recovery temperature) is defined by the film cooling effectiveness parameter per Eq. (1). The local mixed velocity, V_M, was then defined by a similar parameter and also set equal to η:

$$\frac{(V_G - V_M)}{(V_G - V_C)} = \frac{(T_G - T_{aw})}{(T_G - T_C)} = \eta \quad (13)$$

Where V_G is the local hot gas velocity and V_C is the coolant slot exit velocity.

Rearranging Eq. (13), the mixed velocity is:

$$V_M = V_G - \eta (V_G - V_C) \quad (14)$$

Which means that η is also part of the iterative solution.

Traversing Probes Corrections

Most of the traversing probes data is presented as indicated uncorrected values. Local hot gas driving temperature, T_G, however, was needed for improvements in the film cooling effectiveness correlation. When more accurate local values were needed for correlating data, both radiation and recovery corrections were made to the indicated values because the thermocouple junction was unshielded.

A heat balance similar to the one for the plug wall was used. View factors were also included for the radiation terms because radiation between the thermocouple and the hot plug wall occurred in addition to radiation to ambient conditions. The view factors changed with radial position of the probe. The local hot gas stream velocity was also needed (computed from corrected total pressure probe readings) for determining the convective heat transfer between the hot gas and the thermocouple. Local hot gas Mach numbers were also computed to determine the thermocouple recovery factor.

Results and Discussion

A matrix of the major test variables is presented in Table I. Three data sets were chosen from the overall test matrix to illustrate the trends obtained. The data is first presented with average hot gas temperature and constant recovery factor used in defining the correlation parameters. These plots are then followed by a more detailed look at the flow environment and finally, improved correlations based on local hot gas driving temperature and variable recovery factor along the plug wall are presented.

Overall Film Cooling Effectiveness

The term overall is used to describe the results when the average hot gas temperature and constant recovery factor are used. The first data set shown in Fig. 5 represents subsonic nonafterburning film cooling data with the large primary shroud installed. This configuration, where the primary boat-tail angle is low, directs the hot gas flow nearly parallel to the plug wall (see Fig. 3) which was the closest approximation to a subsonic rig type installation. A range of coolant flows from 0.26 to 1.66 percent of the hot gas flow rate and a range of hot gas Mach number from 0.44 to 0.83 is included.

The subsonic data is grouped reasonably well about the design curve[11] also shown in Fig. 5. The agreement is sufficient such that definitions of effective length and the mixing model used appear adequate for these run conditions. The design curve shown is also included in all the remaining correlation plots as a line of reference.

The second data set (Fig. 6) consists of a series of runs having different nozzle pressure ratios which result in hot gas Mach numbers ranging from 1.1 to 2.6. The supersonic hot gas stream overexpands along the plug wall which results in oblique shocks. These data were obtained without afterburning with the small primary shroud which directs the hot gas flow toward the plug at a greater angle than the large primary shroud. The larger data spread in Fig. 6 is the result of shocks, in addition to the flow angle effect. The greatest deviation from the design curve occurs downstream from the location of the first shock that occurs downstream from the cooling slot.

The third data set was selected from partial afterburning runs and covered a range of nozzle pressure ratios and several coolant flow rates at a pressure ratio of 8. The very large spread in overall film cooling effectiveness at different pressure ratios is shown in Fig. 7. The large data spread is the combined effect of shocks, and hot gas temperature gradients. These data indicate that use of the design curve for predicting wall temperatures and cooling air requirements on an overall basis would lead to significant errors for afterburning run conditions.

Flow Field Description

A closer examination of the flow field along the external free expansion surface of the plug was needed to understand why the large data spreads occurred especially for the afterburning runs (Fig. 7).

The measured wall static pressures (ratioed to total pressure) and wall temperatures for the runs of Fig. 7 are included in Figs. 8 and 9 where Fig. 8 shows the effect of nozzle pressure ratio and Fig. 9 shows the effect of coolant flow rate.

The wall temperature profile at a pressure ratio of eight (Fig. 8(a)) and the photograph at this pressure ratio (Fig. 10) show a significant change in temperature pattern relative to the pattern at lower pressure ratios. A portion of the wall temperature profile showed a decrease instead of the typical increase with length from the cooling slot. Additional exploratory tests were run at this pressure ratio (NPR = 8) to determine a minimum cooling flow. The resulting wall temperature profiles are shown in Fig. 9. The plug wall remained relatively cool with high overall film cooling effectiveness (Fig. 7) for reductions in coolant flow down to 0.25 percent of hot gas flow. This flow is near the low limit for convention cooling of the supporting struts and forward end of the plug. Note that the wall temperatures near the middle of the plug for the two lowest coolant flows were less than the coolant temperature at the slot. This is due to the very effective film cooling plus radiation cooling.

The change in temperature pattern is associated with a change in the boundary layer region in the presence of shocks. An indication of the location of shocks may be seen in the wall static pressure profiles (Fig. 8(b)) as well as the photographs (Fig. 10). The static wall pressures decrease downstream from the nozzle throat and then rise downstream from the point of intersection of oblique shocks with the cooling film. The pressure profile and shock location change with nozzle pressure ratio; the shock moving downstream as pressure ratio increases. The solid symbols in Figs. 8 and 9 represent the first measurement station downstream of the first shock location.

Another factor that has an effect on temperature pattern is the large radial hot gas temperature gradients that exist when the afterburner is operating. These gradients were measured with the traversing thermocouple probe and the effect of nozzle pressure ratio on the profiles at an axial position of X = 15 inches is shown in Fig. 11. At low pressure ratios, the maximum T_G (greater than $\overline{T_7}$) is near the plug wall, which results in high wall temperatures and the very low overall effectiveness values in Fig. 7. At high pressure ratios, however, the peak is several inches further away, the flow having turned outward away from the plug. The temperature of the hot gas near the wall is much lower resulting in lower wall temperatures and the film effectiveness based on average hot gas temperatures shows the very high values in Fig. 7.

A more complete description of the flow field was obtained by traversing across the hot gas stream with both total pressure and temperature probes at four downstream positions and one upstream position (near the primary shroud lip) from the cooling slot. These data together with wall static pressures and photographs enables the construction of flow field map approximations which are helpful for interpreting the results obtained. A sample map is shown in Fig. 12. The traversing plane positions are indicating by the vertical straight lines. The indicated temperature and total pressure measured along these radial lines are shown adjacent to each line (labeled at X = 15 in.). An inflection point occurs in the total pressure trace when the probe passes through a shock. These inflections together with the static wall pressure profile and photographs enable an estimate of the location of the oblique shocks (and reflections) to be drawn. The boundary between hot gas and the cooling air film and the separated flow region are also estimated from the pressure and temperature measurements near the plug wall.

The data clearly indicated that at a pressure ratio of 8, a flow separation existed at 15 inches from the cooling slot. This station is downstream from the oblique-shock intersection with the cooling air film (Fig. 12), and probably results from a shock boundary-layer interaction. There was probably recirculation in this zone (P_T less than local P_S on the wall). The separated flow region also was relatively cool (Fig. 11) which suggests that the low velocity separated flow region was filled with film cooling air. Containment of cool air in the separated flow region prevented the wall temperature from rising significantly even at very low cooling flow rates. This phenomena can explain why the effectiveness in Fig. 7 for a pressure ratio of 8 was independent of cooling flow rate over the range tested.

The total pressure traces also showed evidence of a thickening of the boundary layer (no separa-

tion) after passing through another shock-boundary-layer intersection further upstream. Thickening of the boundary layer also had the effect of increasing the film cooling effectiveness on an overall basis.

Experimental Recovery Factors

Good results for correlating film cooling effectiveness data in supersonic flow was obtained[9] when the hot gas driving temperature was obtained experimentally by isoenergetic injection. (Isoenergetic injection implies that the secondary (cooling air) gas is neither heated nor cooled and should have the same total temperature as the main air flow.) This is accomplished in rig tests with low temperature levels and setting coolant temperature equal to hot gas temperature and measuring the adiabatic wall temperatures along the length to be film cooled. The aerodynamic flow effects (hot gas and coolant) including the effects of shocks, etc., are therefore, taken into account. This technique, however, is difficult in engine tests and impossible at afterburning conditions.

An approximation to the isoenergetic approach can be made, however, by tests with no cooling flow from the coolant slot.[8] Flow conditions near the slot would be different, but further downstream the flow environment would probably not be greatly different. Zero-cooling-flow wall-temperature data, of course, would have to be obtained at nonafterburning conditions. The results obtained, however, can be applied to afterburning runs if the adiabatic wall temperature is assumed to be equal to recovery temperature which is defined by Eq. (3) where the recovery factor, R, is defined by Eq. (4). That is, R at each measuring station is determined from nonafterburning, zero cooling flow runs for the same nozzle pressure ratio and used in Eq. (3) for afterburning runs to obtain the hot gas driving temperature $T_{RG(n)}$.

Typical experimental Recovery Factors determined by the method outlined above are presented in Fig. 13. The values vary considerably from the theoretical flat plate value of the cube root of Prandtl number. The marked effect of configuration and operating condition is shown. The method provides a useful calibration technique to correct for the various boundary layer conditions that exist in the supersonic flow field with shocks. Significant improvements in correlating film cooling effectiveness, as described in the next section, was partially due to this technique.

Local Film Cooling Effectiveness

The term local is used to describe the results when a local hot gas driving temperature, $T_{RG(n)}$ is used which includes the correction for local Recovery Factor.

The separate effects of Recovery Factor and a local total temperature obtained from traverse measurements on film cooling effectiveness are shown for a typical run in Fig. 14. The top curve (at $X_{eff}/MS \sim 200$) is the overall effectiveness based on average hot gas temperature, $\overline{T_7}$ and a constant recovery factor of 0.89. The next lower curve is also based on $\overline{T_7}$ but used with variable recovery factors obtained from a zero coolant flow run at the same nozzle pressure ratio. The lowest curve (near the design curve) is based on local hot gas total temperatures obtained from temperature probe traverses (interpolated for intermediate stations and extrapolated for stations downstream of last traversing station) plus the application of local recovery factors. The local temperatures were obtained by correcting indicated values at one inch from the plug wall. (The choice of one inch is rather arbitrary, but seemed to improve the correlation better than a lesser or greater distance.)

Although the run shown in Fig. 14 is a nonafterburning condition where the hot gas temperature profile at the nozzle throat is relatively flat, local temperature gradients through the cooling film and nearby hot gas stream were sufficient to significantly affect the effectiveness parameter, which is sensitive to the hot gas driving temperature. The flow is separated downstream of the shock for the run shown and the fit of the corrected data may be fortuitous in that data in the separated flow region of other runs did not correlate. In general, data obtained with the small primary shroud had large recovery factor corrections relative to local hot gas temperature corrections whereas the afterburning runs had large temperature corrections relative to recovery factor corrections.

A typical subsonic run from each of the two primary shrouds used were corrected for local recovery factor and local temperature and are compared in Fig. 15. The small primary, which directs the flow at a greater angle to the plug wall has a higher film cooling effectiveness than the large primary at high values of X/MS. The reason for this is not known, but it illustrates that film cooling may be sensitive to configuration variables.

Several runs having different nozzle pressure ratios were processed using local hot gas temperature and variable recovery factors. The data for nonafterburning with the small primary shroud is shown in Fig. 16. Some improvement in the data spread is noted as compared to the overall effectiveness in Fig. 6. The high pressure ratio run, however, was over corrected for data downstream of the shock in the separated flow region. The overcorrected data are not shown.

The data corrected for local conditions with the afterburner operating (Fig. 17) shows a large improvement compared to the overall effectiveness in Fig. 7. In this case accounting for the large temperature gradients during afterburning had the most pronounced effect on correlation improvements. Again, the data in the separated flow region has large deviations and are not shown. Evidence of data point deviations from the main data group for nonseparated but thickened boundary layer regions downstream of shocks also appear in both Figs. 16 and 17. The results indicate the need for improved mixing models for film cooling in the presence of shocks especially when flow separation is present. An improved definition of hot gas driving temperature is also needed.

Concluding Remarks

Although some of the factors causing the poor data correlation using overall conditions have been identified, and used to improve the correlation, the application of the improved correlation for design purposes requires inputs that may not be readily available.

Local recovery factors in the supersonic flow with shocks environment are difficult to predict theoretically. The possibility exists, however, that these may be determined by simple nozzle experiments, perhaps with accurate scale models, that are instrumented for temperatures as well as pressures.

Predicting the local hot gas driving temperature may be even more difficult than predicting local recovery factors. The values of local temperature reflects the combined effect of temperature gradients produced by the afterburner, flow turning within the nozzle (effect of transition sections), flow turning through shock waves, and mixing with film cooling air in the boundary-layer. What happens in flow separation regions is not well understood. It is not known whether the cool air pocket "trapped" in the separation region of this experiment will happen in nonaxisymmetric nozzles where 3D flow phenomena may affect it differently.

Additional analysis of the data acquired in this test program may lead to an improved definition of what the hot gas driving temperature should be.

Summary of Results

Exploratory tests with a film-cooled external-expansion axisymmetric plug nozzle behind an afterburning turbojet engine in an altitude test facility produced the following results:

1. An existing film-cooling-effectiveness versus a length parameter correlation was adequate for correlating data at nonseparated flow conditions provided that local recovery factors and local hot gas driving temperatures are used. Different design curves, however, may be needed for different nozzle configurations.

2. Use of an effective length for a nonflat-plate geometry produced satisfactory results.

3. Overall film cooling effectiveness in separated flow regions was high and independent of cooling flow rate over the range tested at nozzle pressure ratios above 7 for the geometry investigated.

References

1. Berrier, B. L., Palcza, J. L., and Richey, G. K., "Nonaxisymmetric Nozzle Technology Program - an Overview," AIAA paper 77-1225, Aug. 1977.

2. Schnell, W. C., Grossman, R. L., and Hoff, G. E., "Comparison of Nonaxisymmetric and Axisymmetric Nozzles Installed on a V/STOL Fighter Model," SAE paper 770983, Nov. 1977.

3. Capone, F. J., Gowadia, N. S., and Wooten, W. H., "Performance Characteristics of Nonaxisymmetric Nozzles Installed on the F-18 Airplane," AIAA paper 79-0101, Jan. 1979.

4. Nosek, S. M., and Straight, D. M., "Heat Transfer Characteristics of a Partially Film-Cooled Plug Nozzle on a J85 Afterburning Turbojet Engine," NASA TM X-3362, 1976.

5. Graber, E. J., Jr. and Clark, J. S., "Comparison of Predicted and Experimental Heat-Transfer and Pressure-Drop Results for an Air-Cooled Plug Nozzle and Supporting Struts," NASA TN D-6764, 1972.

6. Chenoweth, F. C. and Lieberman, A, "Experimental Investigation of Heat-Transfer Characteristics of a Film-Cooled Plug Nozzle with Translating Shroud," NASA TN D-6160, 1971.

7. Hatch, J. E. and Papell, S. S., "Use of a Theorectical Flow Model to Correlate Data for Film Cooling or Heating an Adiabatic Wall by Tangential Injection of Gases of Different Fluid Properties," NASA TN D-130, 1959.

8. MuKerjee, T. and Marten, B. W., "Film Cooling by Air Injection Through a Backward-Facing Annular Tangential Slot into a Supersonic Axisymmetric Parallel Diffuser," Proceedings of the 1968 Heat Transfer and Fluid Mechanics Institute, A. F. Emery and C. A. Depew, eds., Stanford Univ. Press, Stanford, Calif., 1968, pp. 221-242.

9. Goldstein, R. J., Eckert, E. R. G., Tsou, F. K., and Haji-Sheikh, A., "Film Cooling with Air and Helium Injection Through a Rearward-Facing Slot into a Supersonic Air Flow," AIAA J., Vol. 4, June 1966, pp. 981-985.

10. Juhasz, A. J. and Marek, C. J., "Combustor Liner Film Cooling in the Presence of High Free-Stream Turbulence," NASA TN D-6360, 1971.

11. Konarski, M. and Clayton, T., "J85 Nonaxisymmetric Nozzle Design and Cooling Study," General Electric Co., Cincinnati, Ohio, June 1978 (NASA CR-135289).

12. Samanich, N. E., "Flight Investigation of an Air-Cooled Plug Nozzle with an Afterburning Turbojet," NASA TM X-2607, 1972.

13. Turner, R. L., Addie, A. N., and Zimmerman, R. H., "Charts for the Analysis of One-Dimensional Steady Compressible Flow," NACA TN 1419, 1948.

14. Goldstein, R. J., "Film Cooling," Advances in Heat Transfer, Vol. 7, Academic Press, New York, 1971, pp. 321-379.

15. Baker, P. J. and Martin, B. W., "Heat Transfer in Supersonic Separated Flow Over a Two-Dimensional Backward-Facing Step," International Journal of Heat and Mass Transfer, Vol. 9, Oct. 1966, pp. 1081-1088.

16. Clark, J. S. and Lieberman, A., "Thermal Design Study of an Air-Cooled Plug-Nozzle System for a Supersonic Cruise Aircraft," NASA TM X-2475, 1972.

17. Schlichting, H., Boundary-Layer Theory, 6th ed., McGraw-Hill, New York, 1968, pp. 703-705.

TABLE I. - TEST CONDITIONS

Nozzle pressure ratio, P_{T2}/P_0	Afterburner off		Afterburner on		
	Average hot gas total temperature, $\overline{T_7}$, $^{\circ}R$				
	1180 Large primary	1750 Small primary	2500 Large primary	3000 Large primary	3400 Large primary
1.8	X[a]	X	X		
2.0	X	X	X		
2.5		X	X	X	
3.0	X	X	X	X	X
3.5		X	X	X	
4.0	X	X	X	X	
4.5	X	X	X	X	X
5.0	X	X	X	X	
6.0		X	X	X	
8.0	X	X	X	X	X
10.0		X	X		
	Range of coolant flow rates, percent of W_G				
	0 to 1	0 to 5	¼ to 2	1 to 3½	2 to 5
	Engine inlet airflow, W_A, lb/sec				
	28 to 41	20 to 41	21	21	21

[a]X represents conditions where data was obtained.

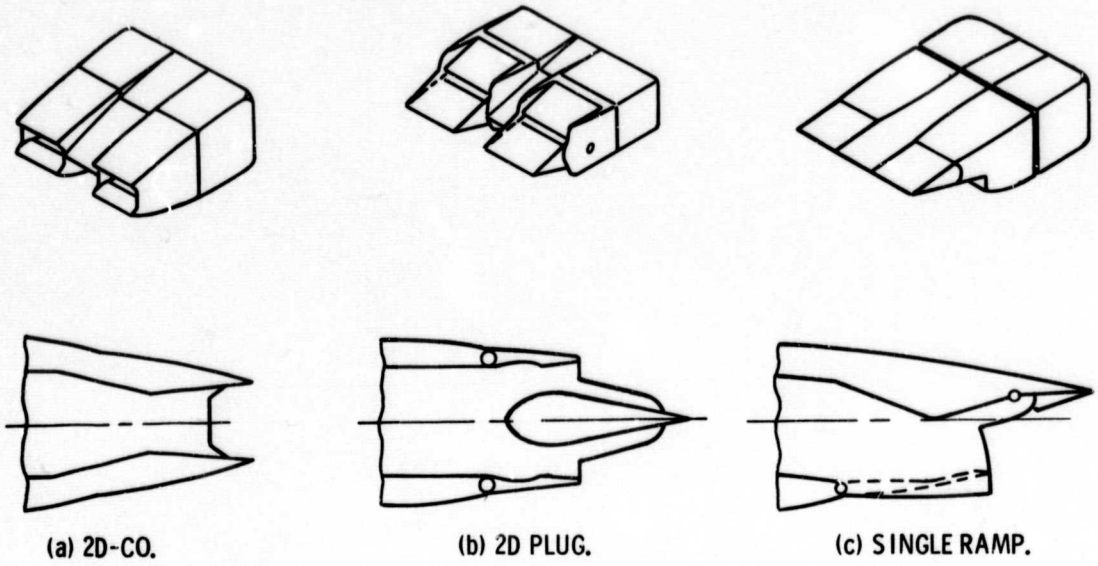

Figure 1. - Three basic types of nonaxisymmetric exhaust nozzles.

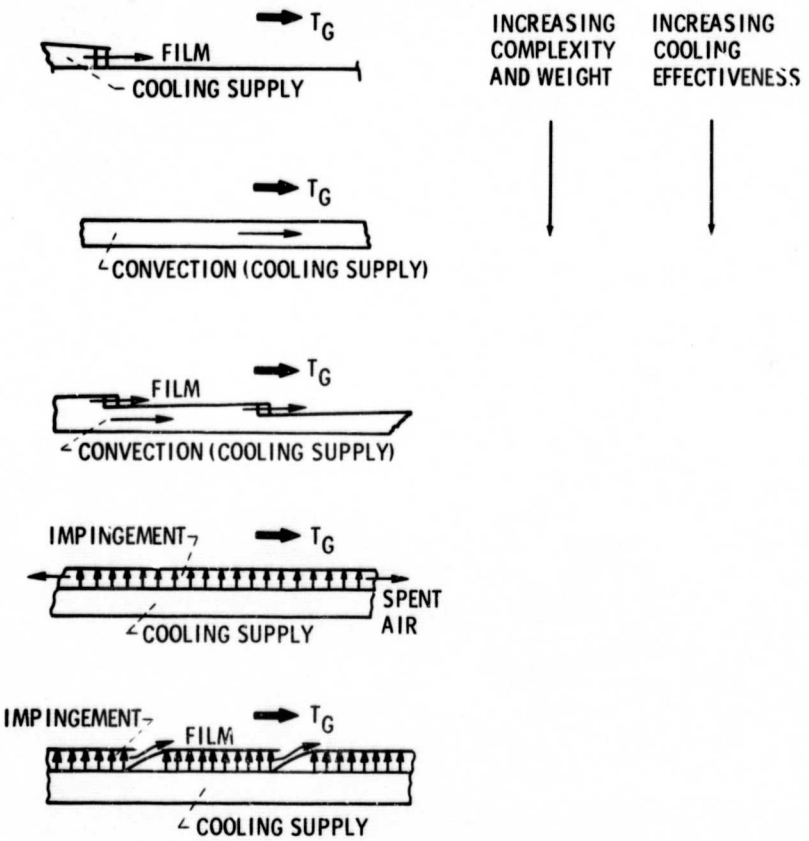

Figure 2. - Cooling methods being considered for nonaxisymmetric exhaust nozzles.

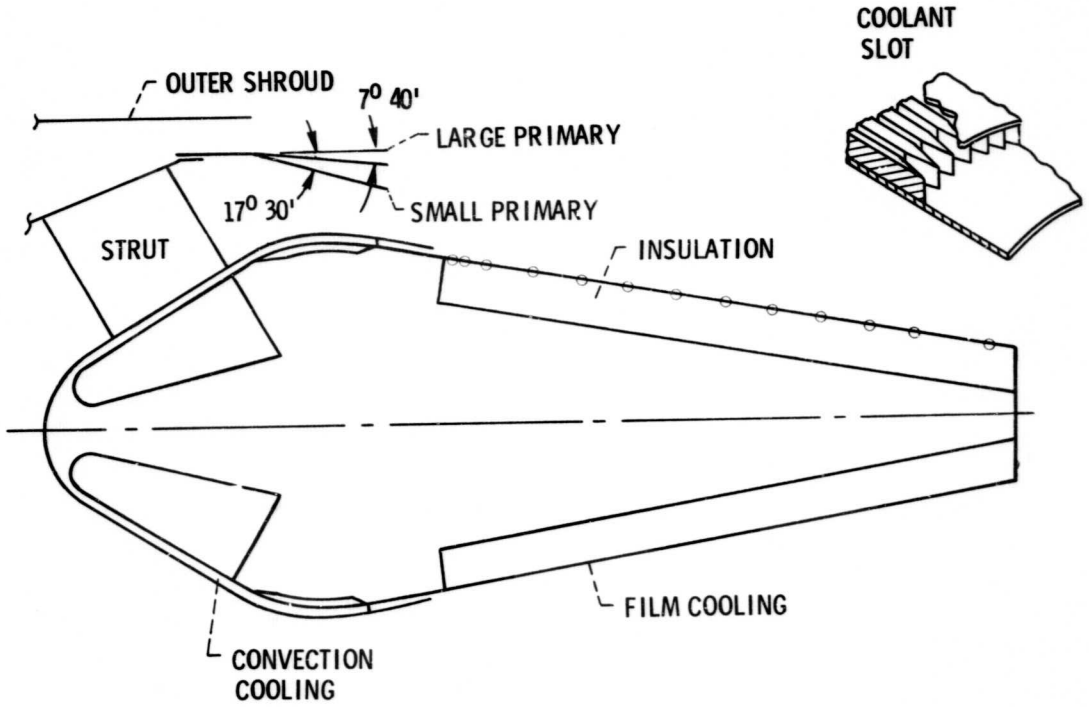

Figure 3. - Schematic of film cooled axisymmetric plug nozzle.

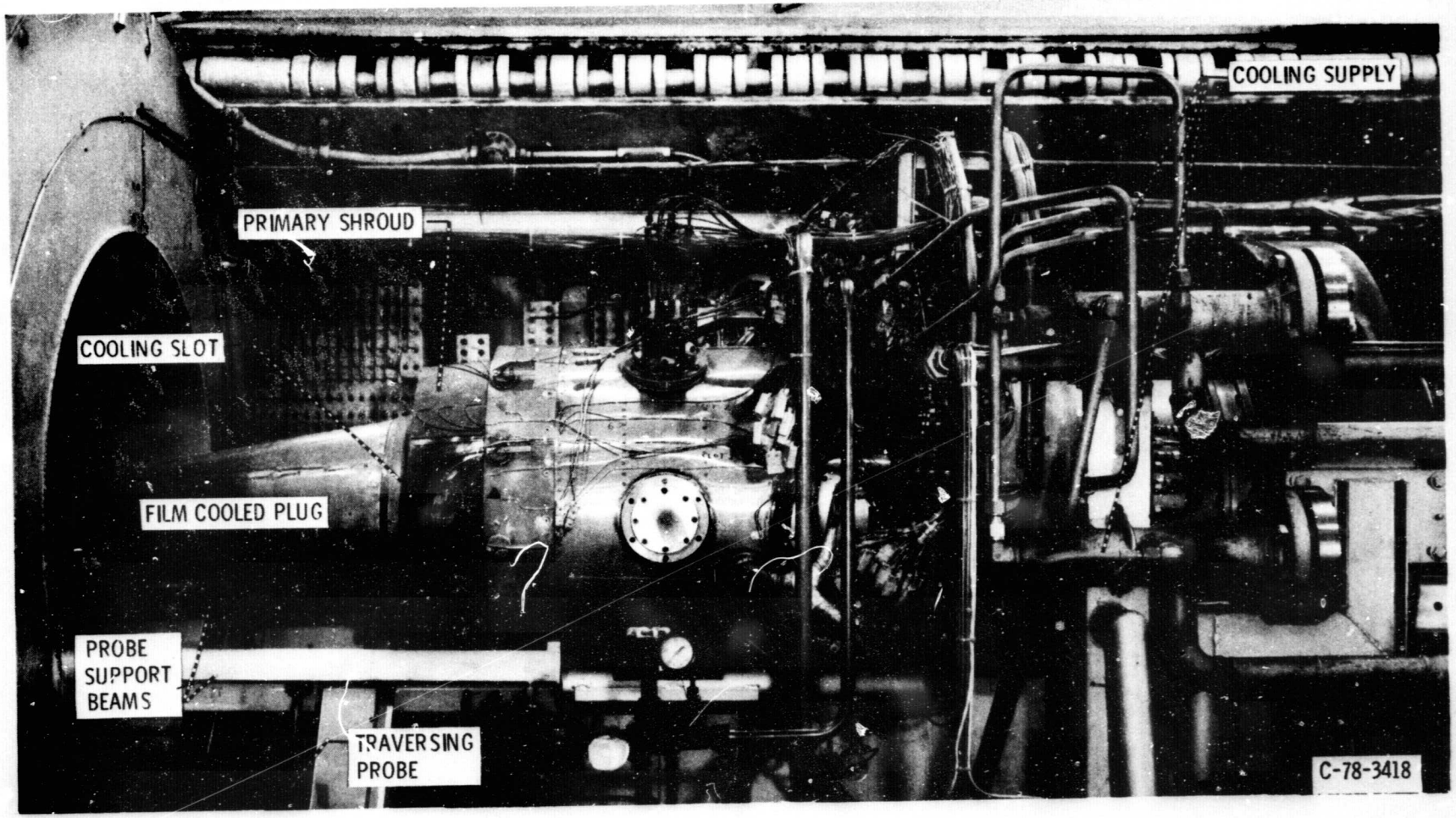

Figure 4. - Installation of axisymmetric film cooled plug nozzle in altitude test facility.

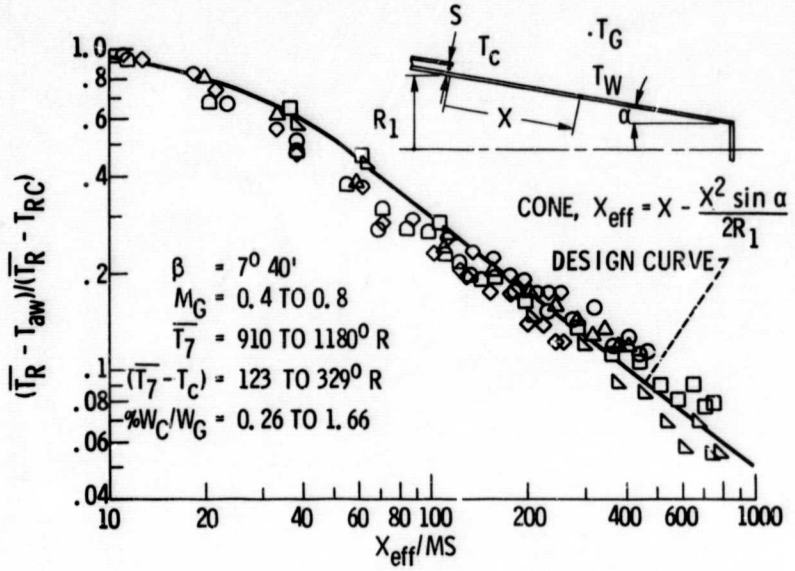

Figure 5. - Comparison of subsonic nonafterburning film cooling effectiveness with reference design curve; large primary shroud on axisymmetric plug nozzle.

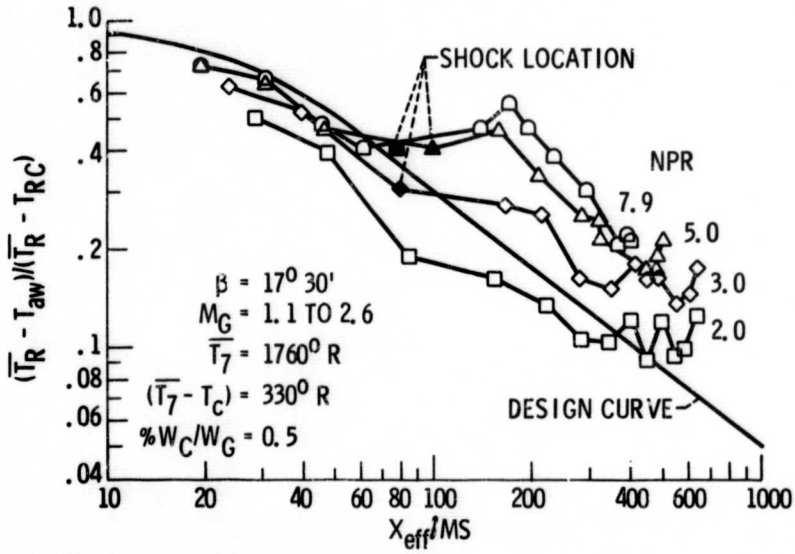

Figure 6. - Effect of nozzle pressure ratio on film cooling effectiveness using average hot gas conditions; nonafterburning, small primary shroud.

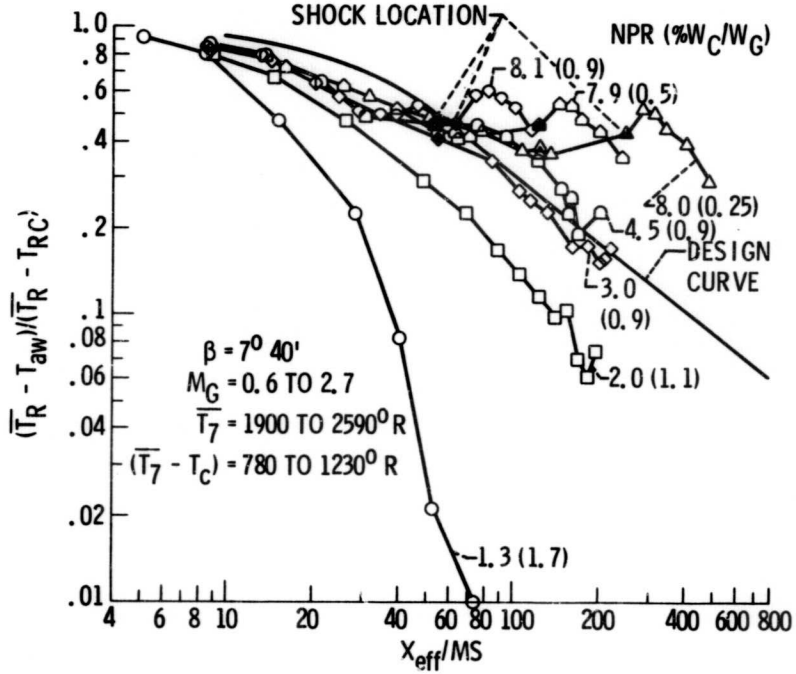

Figure 7. - Effect of nozzle pressure ratio and coolant flow rate on film cooling effectiveness using average hot gas temperature and constant recovery factor; partial afterburning, large primary shroud.

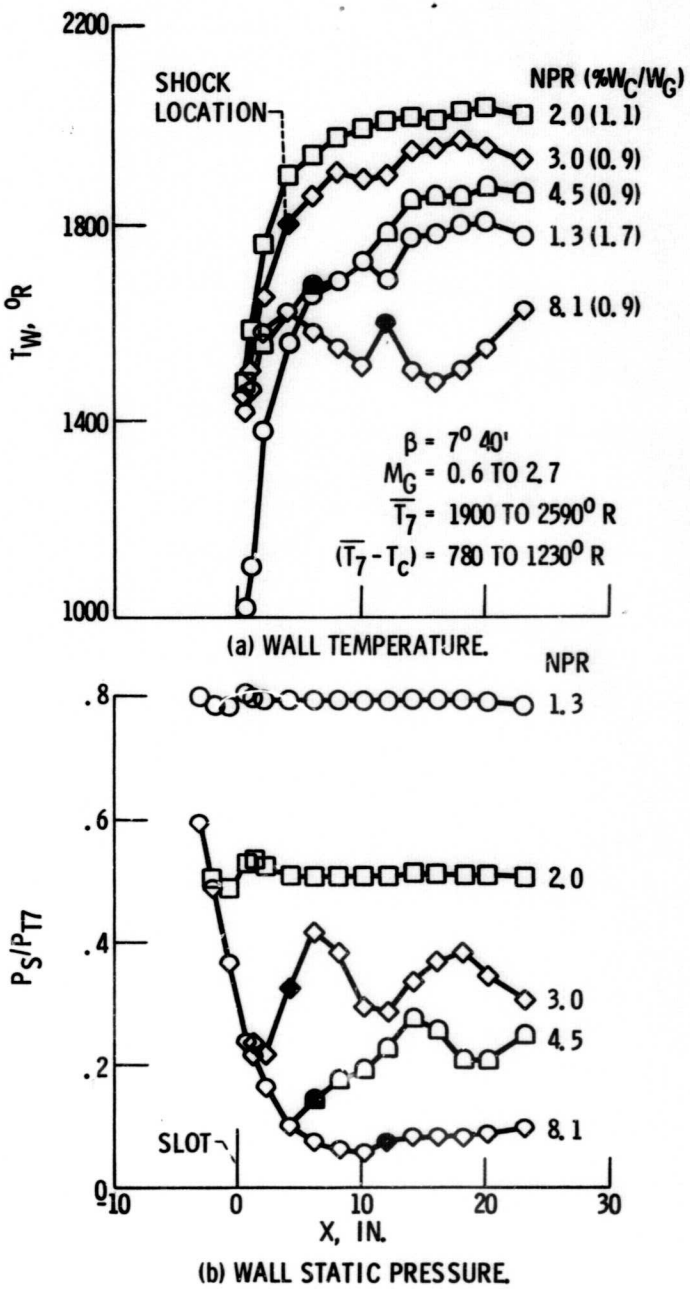

Figure 8. - Effect of nozzle pressure ratio on wall temperature and pressure profiles; partial afterburning with large primary.

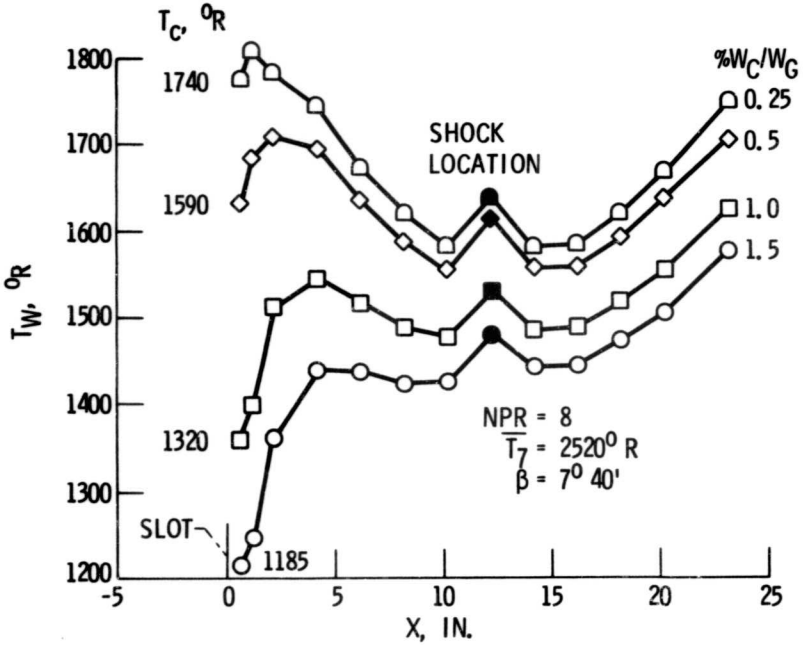

Figure 9. - Effect of coolant flow rate on wall temperature profiles at a nozzle pressure ratio of 8; partial afterburning with large primary shroud.

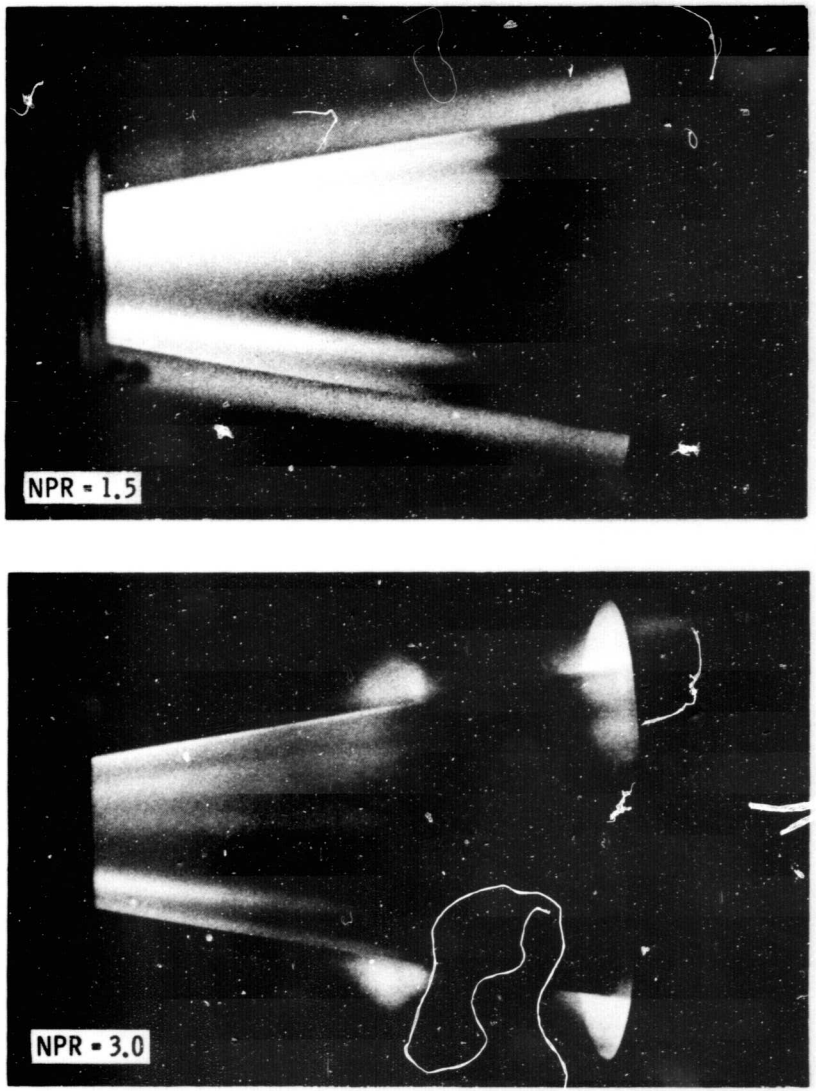

Figure 10. - Plug nozzle operating with afterburning at several nozzle pressure ratios showing shocks and wall temperature patterns.

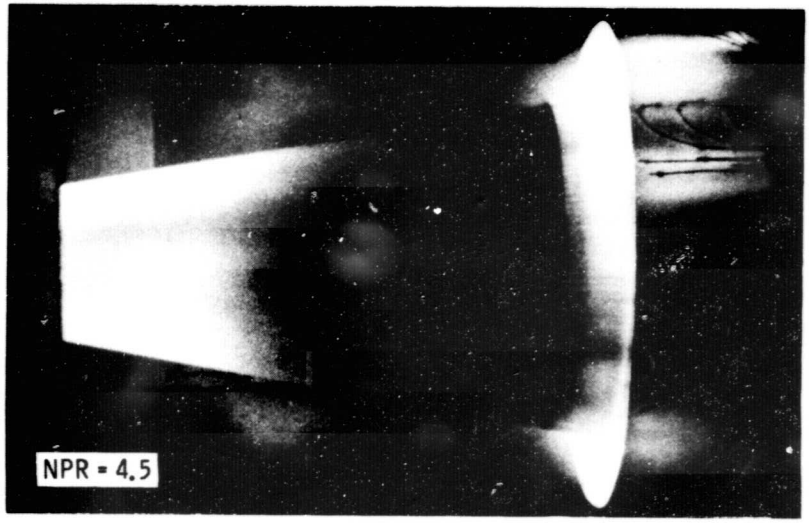

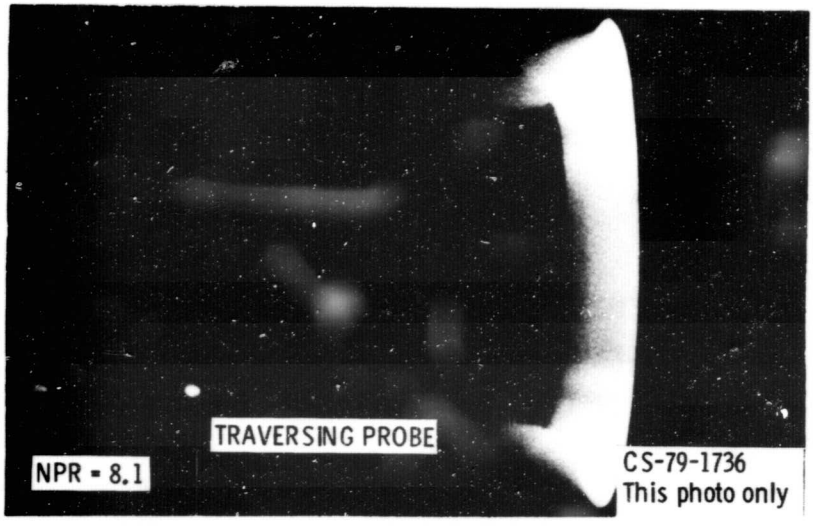

Figure 10. - Concluded.

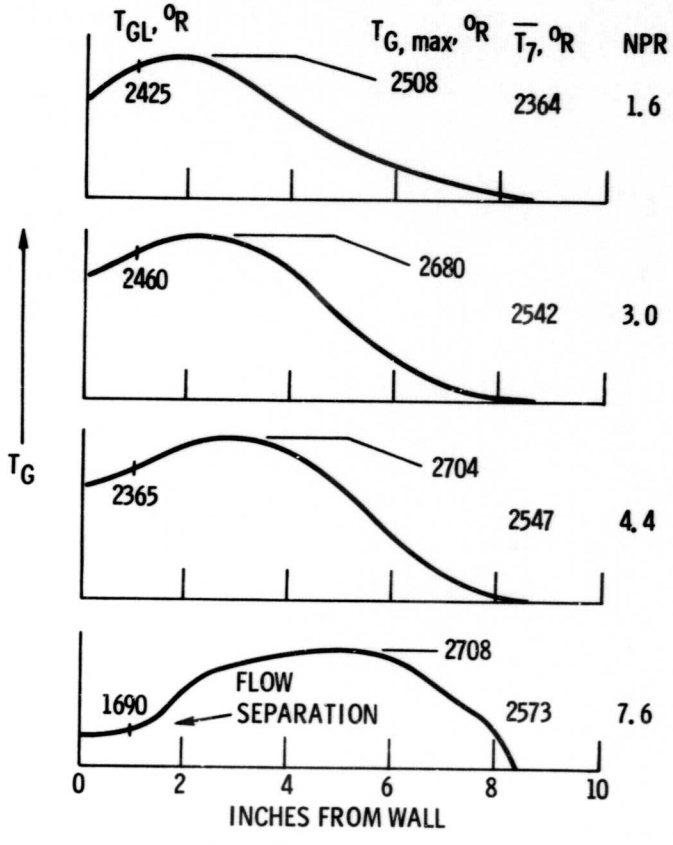

Figure 11. - Traces from on-line records of radial hot gas temperature profiles obtained with traversing thermocouple probe 15 inches downstream from cooling slot.

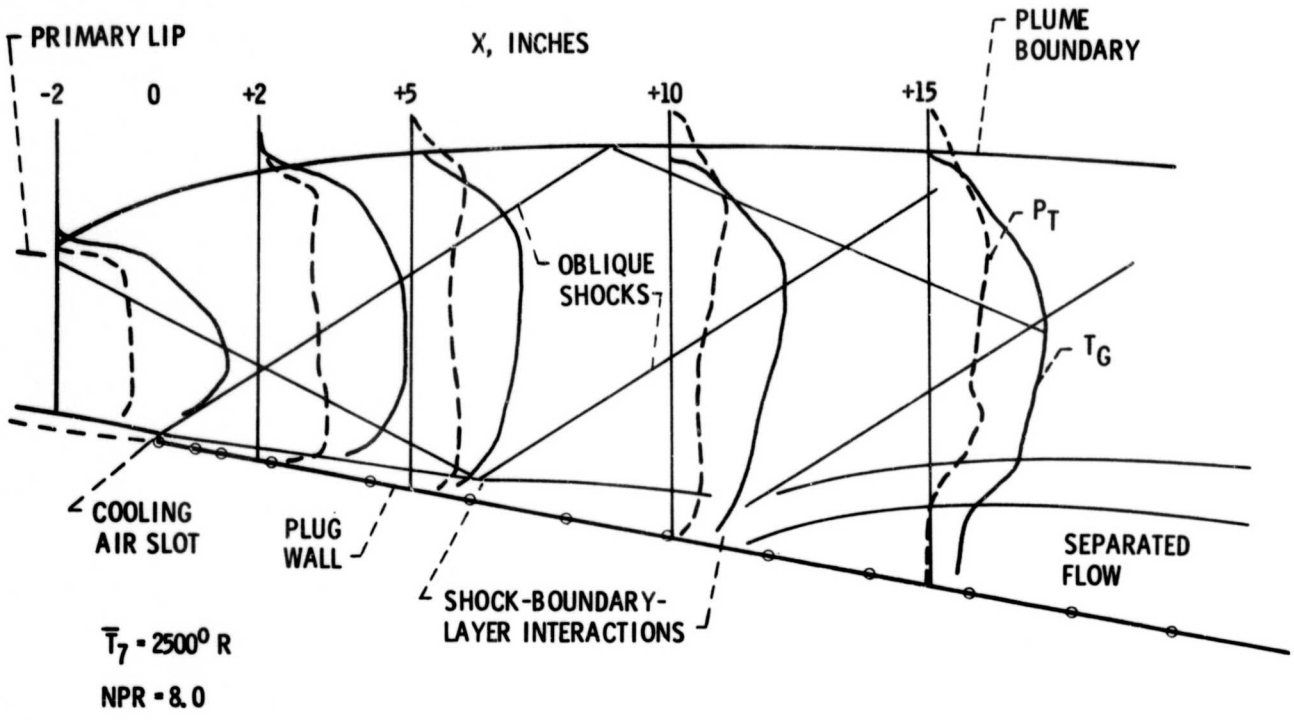

Figure 12. - Free expansion flow field approximation constructed from total pressure and temperature traces of on-line records from traversing probes.

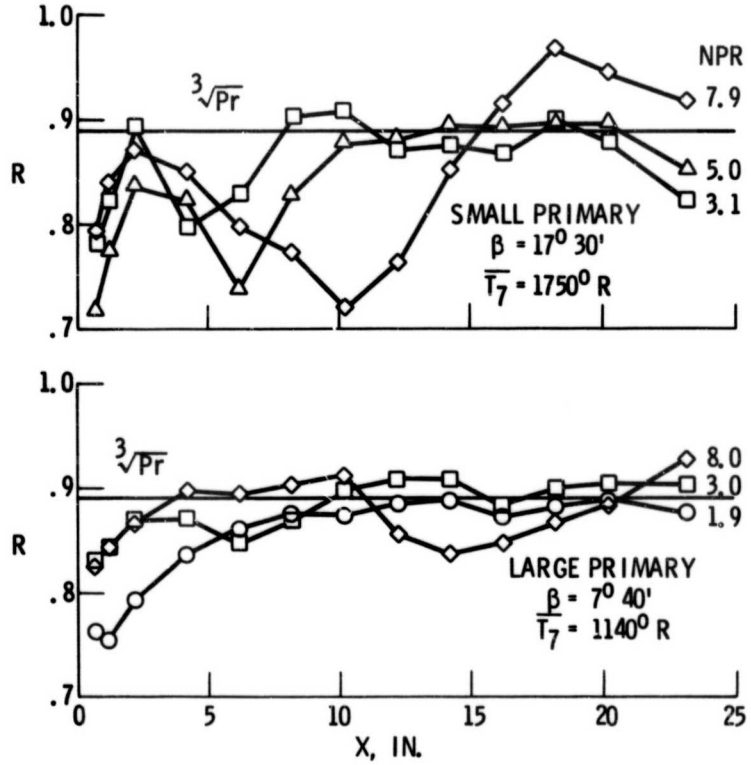

Figure 13. - Effect of nozzle pressure ratio and configuration on local recovery factor along plug wall; zero coolant flow.

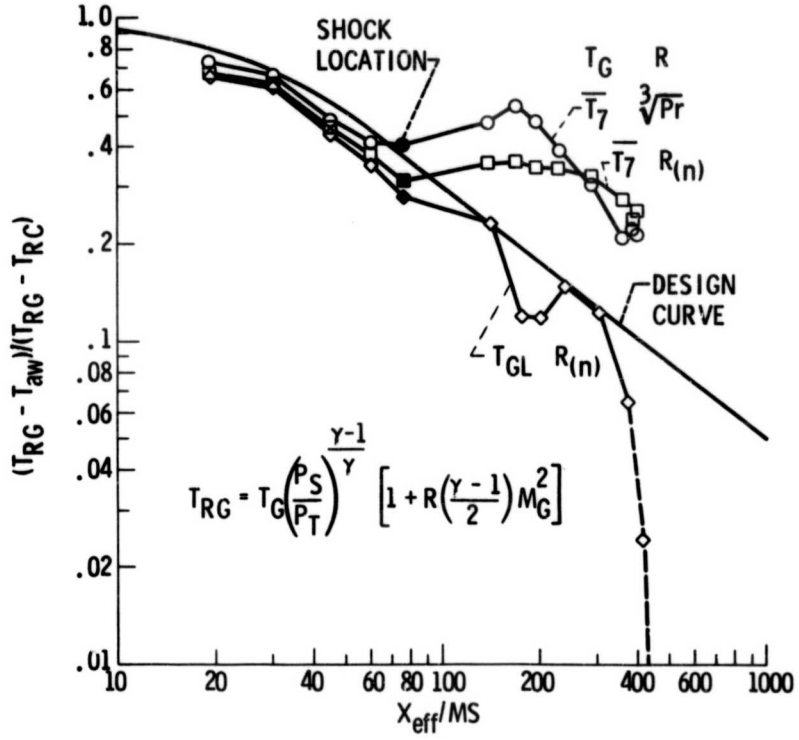

Figure 14. - Development of local film cooling effectiveness parameter, nonafterburning with small primary shroud at nozzle pressure ratio of 7.9.

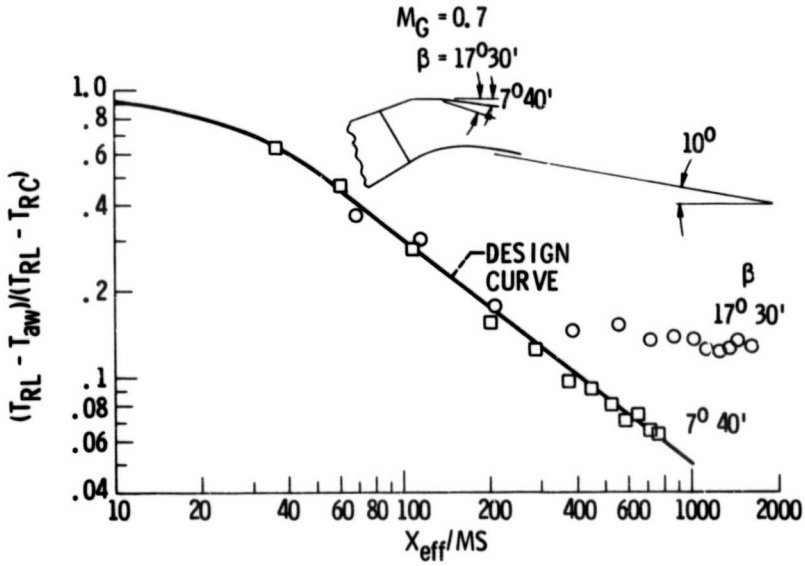

Figure 15. - Effect of primary shroud configuration on subsonic nonafterburning film cooling effectiveness.

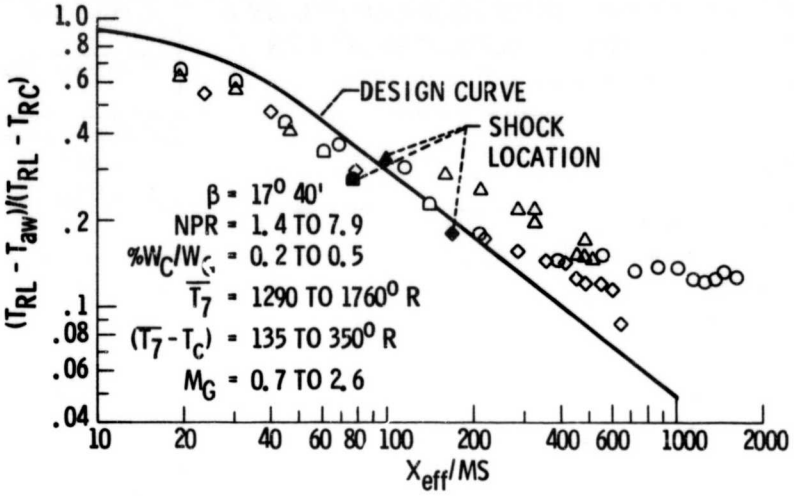

Figure 16. - Correlation of nonseparated-flow film cooling data using local hot gas temperature and variable recovery factor over a range of nozzle pressure ratios; nonafterburning with small primary shroud.

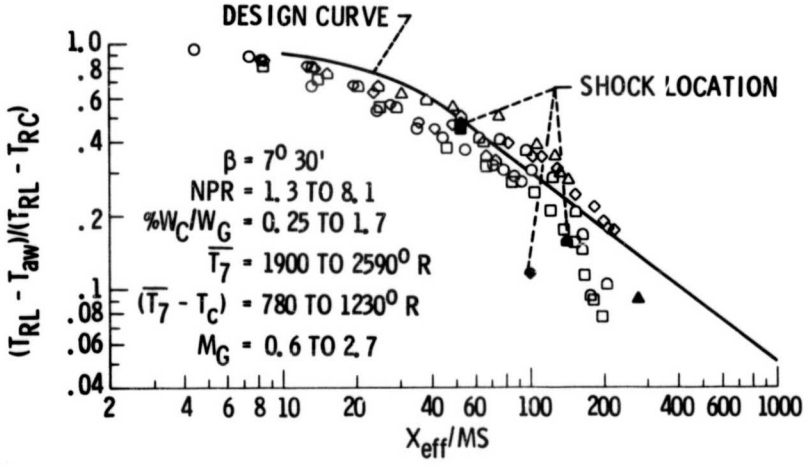

Figure 17. - Correlation of nonseparated-flow film cooling data using local hot gas temperature and variable recovery factor over a range of nozzle pressure ratios and coolant flow rates, partial afterburning with large primary shroud.

1. Report No.	2. Government Accession No.	3. Recipient's Catalog No.
NASA TM-79157		

4. Title and Subtitle	5. Report Date
EFFECT OF SHOCKS ON FILM COOLING OF A FULL SCALE TURBOJET EXHAUST NOZZLE HAVING AN EXTERNAL EXPANSION SURFACE	6. Performing Organization Code

7. Author(s)	8. Performing Organization Report No.
David M. Straight	E-013
	10. Work Unit No.

9. Performing Organization Name and Address	11. Contract or Grant No.
National Aeronautics and Space Administration Lewis Research Center Cleveland, Ohio 44135	

12. Sponsoring Agency Name and Address	13. Type of Report and Period Covered
National Aeronautics and Space Administration Washington, D.C. 20546	Technical Memorandum
	14. Sponsoring Agency Code

15. Supplementary Notes

16. Abstract

Cooling is one of the critical technologies for efficient design of exhaust nozzles, especially for the developing technology of nonaxisymmetric (2D) nozzles for future aircraft applications. Several promising 2D nozzle designs have external expansion surfaces which need to be cooled. Engine data are scarce, however, on nozzle cooling effectiveness in the supersonic flow environment (with shocks) that exists along external expansion surfaces. This paper will present experimental film cooling data obtained during exploratory testing with an axisymmetric plug nozzle having external expansion and installed on an afterburning turbojet engine in an altitude test facility. The data obtained shows that the shocks and local hot gas stream conditions have a marked effect on film cooling effectiveness. An existing film cooling correlation is adequate at some operating conditions but inadequate at other conditions such as in separated flow regions resulting from shock-boundary-layer interactions.

17. Key Words (Suggested by Author(s))	18. Distribution Statement
Exhaust nozzles; Film cooling; Supersonic heat transfer; Plug nozzles; Separated flow	Unclassified - unlimited STAR Category 07

19. Security Classif. (of this report)	20. Security Classif. (of this page)	21. No. of Pages	22. Price*
Unclassified	Unclassified		

* For sale by the National Technical Information Service, Springfield, Virginia 22161